Supervised Learning-enhanced Multi-Group Actor Critic for Live-stream Recommendation

Liu Jingxin
Kuaishou Technology
Beijing, China
liujingxin05@kuaishou.com

Gao Xiang
Kuaishou Technology
Beijing, China
gaoxiang12@kuaishou.com

Li YiSha
Kuaishou Technology
Beijing, China
liyisha@kuaishou.com

Li Xin
Kuaishou Technology
Beijing, China
lixin05@kuaishou.com

Lu Haiyang
Kuaishou Technology
Beijing, China
luhaiyang@kuaishou.com

Wang Ben
Kuaishou Technology
Beijing, China
wangben@kuaishou.com

Abstract

Reinforcement Learning (RL) has been widely applied in recommendation systems to capture users' long-term engagement, thereby improving dwelling time and enhancing user retention. In the context of a short video & live-stream mixed recommendation scenario, the live-stream recommendation system (RS) decides whether to inject at most one live-stream into the video feed for each user request. To maximize long-term user engagement, it is crucial to determine an optimal live-stream injection policy for accurate live-stream allocation. However, traditional RL algorithms often face divergence and instability problems, and these issues are even more pronounced in our scenario. To address these challenges, we propose a novel **S**upervised **L**earning-enhanced **M**ulti-**G**roup **A**ctor **C**ritic algorithm (SL-MGAC). Specifically, we introduce a supervised learning-enhanced actor-critic framework that incorporates *variance reduction* techniques, where multi-task reward learning helps restrict bootstrapping error accumulation during critic learning. Additionally, we design a multi-group state decomposition module for both actor and critic networks to reduce prediction variance and improve model stability. Empirically, we evaluate the SL-MGAC algorithm using offline policy evaluation (OPE) and online A/B testing. Experimental results demonstrate that the proposed method not only outperforms baseline methods but also exhibits enhanced stability in online recommendation scenarios.

CCS Concepts

- **Information systems → Recommender systems**; • **Computing methodologies → *Reinforcement learning***.

Keywords

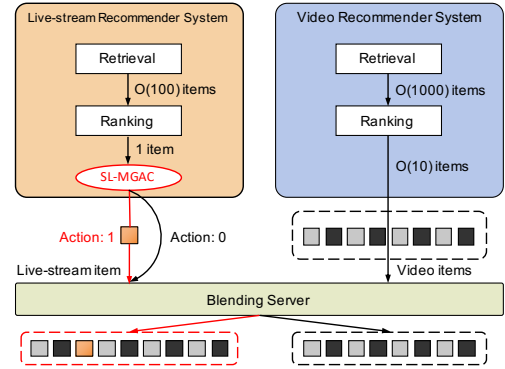Reinforcement Learning, Recommendation System, Variance Reduction

Figure 1: Structure of a short video & live-stream mixed recommendation system(RS). The decision making of SL-MGAC takes place in the final stage of live-stream RS.

1 Introduction

Deep reinforcement learning has shown great potential in learning policies to maximize long-term rewards across various research domains, such as computer vision, robotics, natural language processing, gaming, and recommendation systems [1, 24]. In the context of recommendation systems, reinforcement learning is applied to optimize long-term user engagement [50] and improve user retention [4]. Numerous RL applications have been proposed for real-world recommendation systems, including slate recommendation [8, 18, 27], personalized search ranking [29], and advertisement allocation [25].

We consider a challenging sequential decision-making scenario in a short video & live-stream blended recommendation system, as shown in Fig. 1. The system consists of three components: a live-stream recommendation system, a short video recommendation system, and a blending server. For each user request at timestamp t,

the live-stream recommendation system decides whether to inject the recommended live-stream into the video feed, while the short video recommendation system suggests B (with $B < 10$) videos. The blending server then mixes and rearranges the single live-stream with the B videos to form the final recommendation list. Our objective is to find a personalized optimal live-stream injection policy that maximizes users' long-term engagement with live-streams, which can be modeled as an infinite request-level Markov Decision Process (MDP) [33].

However, the intrinsic issues of divergence and instability associated with traditional reinforcement learning (RL) algorithms [7, 10, 12, 23] are significantly exacerbated in this challenging scenario. A primary possible reason for this is the drastic fluctuations in both the live-stream supply scale and user interaction behaviors over time. As shown in Fig. 2a, the curves of live-stream room count and live-stream viewer count vary significantly on a daily basis, making it difficult for the RL algorithm to learn optimal policies. Furthermore, as illustrated in Fig. 2b, the distributions of user interaction labels (e.g., live-stream and short video watch time) are highly noisy and exhibit large variance. RL models often struggle to learn effective policies from data that exhibit such high variance across both time and user scales. In practice, we observe that RL models frequently encounter issues of *policy deterioration* or *model collapse* [9].
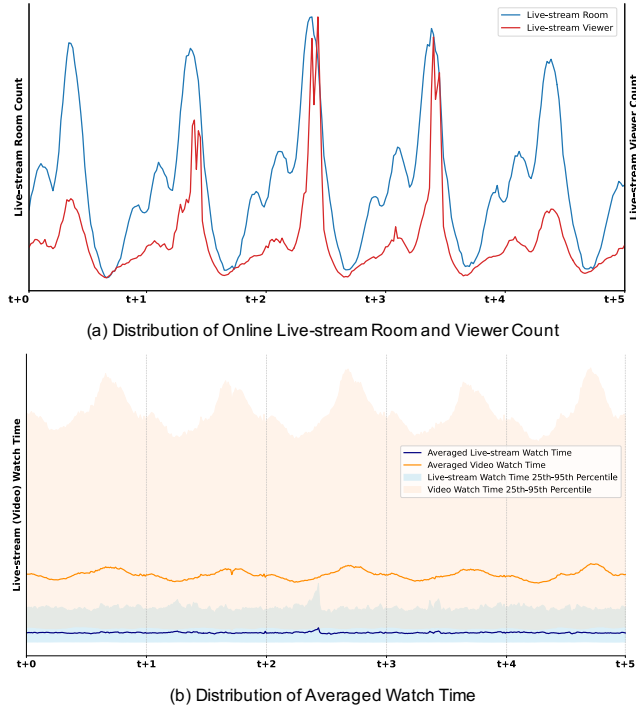

(a) Distribution of Online Live-stream Room and Viewer Count

(b) Distribution of Averaged Watch Time

Figure 2: Data distributions of online live-stream room (or viewer) count, live-stream watch time and short video watch time.

To address the aforementioned issues, we propose a novel Supervised Learning-enhanced Multi-Group Actor Critic algorithm,

SL-MGAC. Given the significant variation in users' interest in live-stream content, which introduces high variance at both the feature and feedback levels, we incorporate separate multi-group state decomposition (MG-SD) modules within both the actor and critic networks. Additionally, we combine multi-task supervised reward learning with traditional critic learning to not only restrict temporal difference (TD) error accumulation during model training but also improve the accuracy of Q-value estimation. Through experiments, we compare the SL-MGAC method with competitive baselines using offline policy evaluation (OPE) [39] and online A/B testing to demonstrate its effectiveness and stability.

The main contributions of this paper are as follows:

- We introduce SL-MGAC, a novel RL model designed to reduce prediction variance while enhancing the stability of both offline training and online inference.
- We propose new *variance reduction* [2, 14, 23, 28, 34] techniques, including multi-group state decomposition, distribution discretization for reward learning, reward normalization, and Q-value normalization.
- We integrate multi-task supervised learning with traditional critic learning to alleviate TD error accumulation and improve the accuracy of Q-value estimation.
- We successfully deploy the SL-MGAC model in a challenging short video and live-stream mixed recommendation scenario for *Kwai*, a short video app with over 100 million users.

2 Problem Formulation

As shown in Fig. 1, in the short video & live-stream mixed recommendation system, the live-stream recommendation system is treated as an agent that interacts with diverse users and receives user feedback over time. The optimal live-stream injection control problem is modeled as an infinite request-level MDP to maximize the cumulative reward. Formally, we define the live-stream injection MDP as a tuple of five elements $(\mathcal{S}, \mathcal{A}, \mathcal{P}, \mathcal{R}, \gamma)$:

- **State space** $\mathcal{S}$: This is the set of user interaction states s, which includes user static features (e.g., user ID, location, gender, country), user history features (e.g., live-stream watch history, short video watch history), and item features (e.g., live-stream ID, author ID, author gender, online viewer count). We limit the length of users' live-stream and short video history lists by timestamp order, keeping only the top 50 items.
- **Action space** $\mathcal{A}$: The action $a \in \mathcal{A}$ represents the decision of whether to inject a recommended live-stream in response to a user's request. We define action a as a binary variable, where $a = 1$ means injecting a live-stream, and $a = 0$ means not injecting it.
- **Transition Probability** $\mathcal{P}$: The transition probability is denoted as $p(s_{t+1}|s_t, a_t)$, determined by the environment.
- **Reward Function** $\mathcal{R}$: The reward function $\mathcal{R}$ is a mapping from state s_t and action a_t at timestamp t, which can be formulated as $r(s_t, a_t) : \mathcal{S} \times \mathcal{A} \rightarrow \mathbb{R}$.
- **Discount Factor** γ: The discount factor $\gamma \in [0, 1]$ is used in the computation of cumulative reward. Typically, we set $\gamma < 1$ during model training.
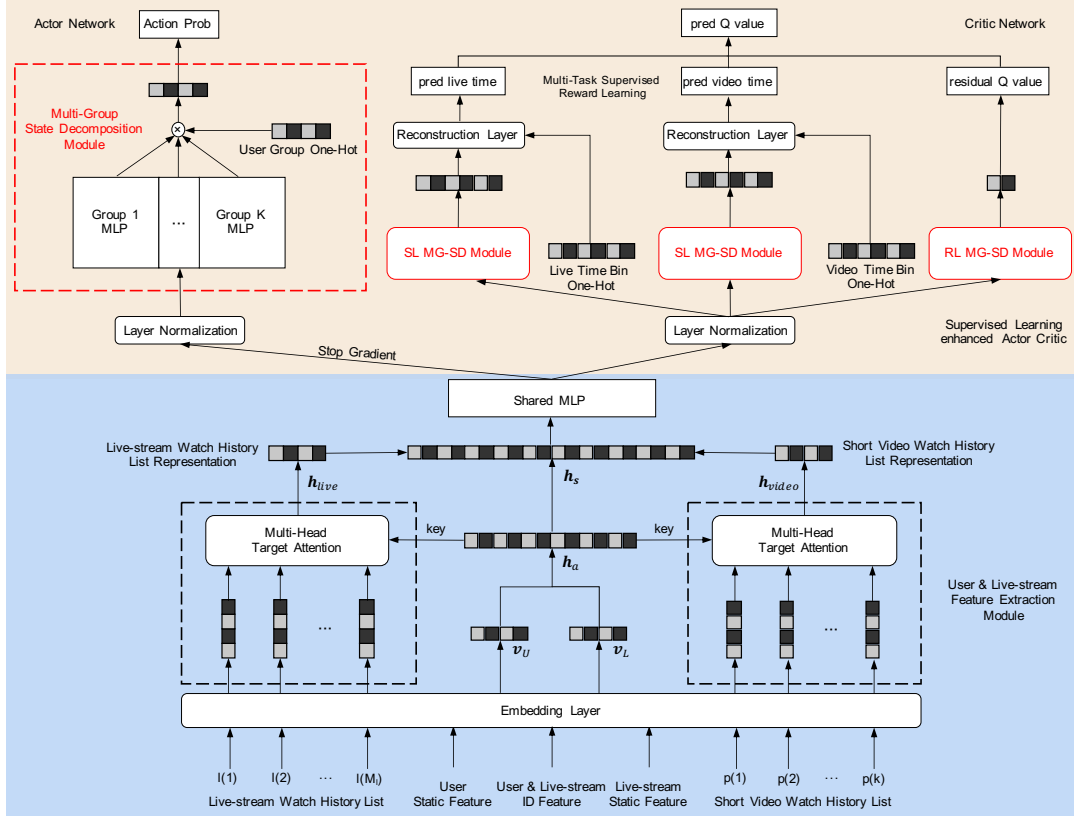
Figure 3: Overall framework of the SL-MGAC algorithm. The SL (RL) MG-SD Module is short for the Multi-Group State Decomposition Module for supervised reward learning and critic learning.

Overall, the optimization objective of aforementioned optimal live-stream injection control problem is shown as follows:

$$\max_{\pi} \mathbb{E}\left[\sum_{t=0}^{\infty} \gamma^t r(s_t, a_t)\right] \quad (1)$$

where $\pi(a_t|s_t)$ is the live-stream injection policy to be optimized.

2.1 Reward Function Design

In our mixed short video & live-stream recommendation scenario, we design a reward function based on the time gain of live-stream watch time relative to the average short video watch time in a request:

$$r(s_t, a_t) = \begin{cases} y_l - \frac{1}{B}y_v, & if\ a_t = 1 \\ \beta & otherwise \end{cases} \quad (2)$$

where y_l is the live-stream watch time, y_v is the total video watch time, B is the number of videos in a request, and β is the hyper-parameter in Eq. 2. Note that the recommended list in a request always contains B videos and at most one live-stream. Furthermore, the reward defined above is similar to that of the RCPO [38] algorithm. From the perspective of constrained reinforcement learning,

the term $\frac{1}{B}y_v$ can be viewed as an implicit cost constraint. In practice, the hyper-parameter β is introduced to carefully control the final live-stream injection ratio.

Since the distribution of live-stream (short video) watch time changes drastically over time, as shown in Fig. 2b, it is challenging for an RL agent to optimize the cumulative reward in Eq. 2. To address this, we propose a reward normalization technique as follows:

$$r(s_t, a_t) = \begin{cases} sigmoid\left(y_l - \frac{1}{B}y_v\right), & if\ a_t = 1 \\ \beta \in [0, 1] & otherwise \end{cases} \quad (3)$$

which helps stabilize the network gradient, thereby reducing the risk of model divergence.

3 Proposed Framework

To address the intrinsic divergence and instability issues of reinforcement learning and successfully deploy the RL agent in our mixed short video & live-stream recommendation system, we propose a novel Supervised Learning-enhanced Multi-Group Actor-Critic algorithm (SL-MGAC), as shown in Fig. 3. SL-MGAC incorporates a supervised learning-enhanced actor-critic model with a shared user & live-stream feature extraction module, along with independent Multi-Group State Decomposition (MG-SD) modules. For clarity, only one critic network is shown in Fig. 3, while the

remaining three critic networks, which use the same architecture, are omitted.

3.1 User & Live-stream Feature Extraction Module

The user & live-stream feature extraction module aims to generate non-linear embedding representations for the state s_t. First, we use a unified embedding layer to map the user's static features, live-stream features, historical live-stream list features and short video list features into low-dimensional dense representations. We denote $\mathbf{v}_U, \mathbf{v}_L, \{\mathbf{e}_1, \cdots, \mathbf{e}_{M_l}\}, \{\mathbf{e}'_1, \cdots, \mathbf{e}'_{M_v}\}$ as the corresponding embedding vectors or sets of embedding vectors, respectively. We then define $\mathbf{h}_a = [\mathbf{v}_U, \mathbf{v}_L]$ as the concatenation of $\mathbf{v}_U$ and $\mathbf{v}_L$.

To aggregate historical live-stream (short video) representations, we introduce the *target attention* mechanism [41, 49], which is defined as follows:

$$\mathbf{h}_{live} = \sum_{i=0}^{M_l} f_l(\mathbf{h}_a, \mathbf{e}_i)\mathbf{e}_i$$
$$\mathbf{h}_{video} = \sum_{j=0}^{M_v} f_v(\mathbf{h}_a, \mathbf{e}'_j)\mathbf{e}'_j \tag{4}$$

where f_l, f_v are different target attention functions, such as a feed-forward network whose output is a normalized score.

After aggregating the historical live-stream and short video features via two separate attention networks, we concatenate all the above embedding vectors to form $\mathbf{h}_s = [\mathbf{v}_U, \mathbf{v}_L, \mathbf{h}_{live}, \mathbf{h}_{video}]$. We then use a shared multi-layer perceptron (MLP) for both the actor and critic networks to obtain the latent representation of state s_t, i.e. $\mathbf{h}'_s = f_{MLP}(\mathbf{h}_s)$. To ensure training stability, we stop the gradient flow through $\mathbf{h}'_s$ for the actor network and only use the more complex critic networks to optimize $\mathbf{h}'_s$, as we find that sharing the feature extraction module and the f_{MLP} network causes interference between the policy and critic gradients.

3.2 Multi-Group State Decomposition Module

Since live-stream content is not equally appealing to all users on the short video app *Kwai*, it is crucial to inject live-streams selectively into the short video feed. Otherwise, excessive live-stream exposures may disrupt a user's interest in short videos, leading to a decrease in overall app usage duration. In practice, user interaction data for live-streams is sparser and noisier compared to that for short videos, making it challenging for RL algorithms to learn an optimal live-stream injection policy for each individual user.

Therefore, prior information about diverse user groups is essential for enhancing the decision-making accuracy of RL models. A natural approach to distinguish between different user behaviors is to partition users into distinct groups based on their historical activity. Specifically, we categorize users into K disjoint groups according to their live-stream activity level, which is determined by the cumulative live-stream watch time over the past 3 weeks. Users with higher historical watch time are assigned to groups with higher activity levels.

Formally, we present the following theorem, which demonstrates that the proposed multi-group state decomposition can be viewed

as a type of *variance reduction* technique for real-world RL applications.

THEOREM 3.1. *Let state space* $\mathcal{S} = \bigcup_{i=1}^{K} \mathcal{S}_i, \forall i \neq j \; \mathcal{S}_i \cap \mathcal{S}_j = \varnothing$, *state* $s \in \mathcal{S}$; r *be the real reward of state* s *and action* a, $\hat{r}$ *be the predicted value of* r *over* $\mathcal{S}$, $\hat{r}_i$ *be the predicted reward of* r *over* $\mathcal{S}_i$; *then a neural network* f *with MG-SD module has a lower prediction variance than the neural network* f' *without MG-SD module.*

Please refer to Appendix. A for detailed proof of Theorem 3.1. We demonstrate that the MG-SD module eliminates between-group variance, thereby reducing the total variance, which implies that the multi-group state decomposition module contributes to a more stable RL model. Empirically, we also show the effectiveness of this module in enhancing RL model stability in subsequent experiments. We find that SL-MGAC without the MG-SD module tends to be more unstable during training, with a larger variance in its Q-values.

3.3 Supervised Learning-enhanced Actor Critic

To alleviate the impact of drastic changes in data distribution that could lead to the divergence or instability of RL models, we propose a supervised learning-enhanced actor critic framework to prevent critic networks from getting trapped in model collapse due to large cumulative errors in the critic learning process.

3.3.1 Layer Normalization. A recent work on RL divergence and instability [45] shows that offline critic learning exhibits a *self-excitation* pattern. Specifically, Q-value iteration can inadvertently cause the target Q value $Q(s_{t+1}, a^*)$ to increase even more than the increment of $Q(s_t, a_t)$, which amplifies the TD-error and traps the critic learning process in a positive feedback loop until model collapse. Therefore, normalization techniques, such as *Layer Normalization* [3] can be utilized to alleviate the divergence and instability problems.

From the proof in the Appendix D of [45], we know that for any input $\mathbf{x}$ and any direction $\mathbf{v}$, if a network applies Layer Normalization to the input, then we have $k_{\text{NTK}}(\mathbf{x}, \mathbf{x} + \lambda\mathbf{v}) \leq C$, where $\lambda > 0$, C is a constant and k_{NTK} is the *Neural Tangent Kernel* (NTK) [19]. This theoretically indicates that a network with Layer Normalization is less sensitive to input variations and can maintain stable gradients despite perturbations during model training. Hence, we apply Layer Normalization to the inputs of both the actor and critic networks, as shown in Fig. 3.

3.3.2 Critic Network. Let $(s_t, a_t, r_t, s_{t+1}, a_{t+1}, r_{t+1}) \in \mathcal{D}$ be a training sample from our real-time dataset $\mathcal{D}$. To address the *maximization bias* problem [40], we employ four critic networks: two current Q-networks Q_{ϕ_1}, Q_{ϕ_2} and two corresponding target Q-networks Q'_{ϕ_1}, Q'_{ϕ_2} in Clipped Double Q-Learning [12]. The critic learning objective is as follows:

$$\mathcal{L}_{Critic} = \sum_{i=1}^{2} \mathbb{E}_{(s,a) \in \mathcal{D}} \left[Q_{\phi_i}(s_t, a_t) - Q_{label}(s_{t+1}) \right]^2$$
$$Q_{label}(s_{t+1}) = r(s_t, a_t) + \gamma \max_{a_{t+1}} \hat{Q}'(s_{t+1}, a_{t+1}) \tag{5}$$

where $\hat{Q}'(s_{t+1}, a_{t+1}) = \min_{i=1,2} Q'_{\phi_i}(s_{t+1}, a_{t+1})$. We use Huber Loss [16] to optimize the above objective.

In practice, $Q_{label}(s_{t+1})$ may be dominated by $\hat{Q}'(s_{t+1}, a_{t+1})$ during critic learning, which can affect the performance of the critic networks. Therefore, we seamlessly introduce supervised learning (e.g. multi-task learning [48]) into the critic learning procedure. Specifically, we split the critic network Q_{ϕ_i} (or Q'_{ϕ_i}) into two components: a Reward Prediction Network (RPN) and a Q Residual Network (QRN), as follows:

$$Q_{\phi_i}(s_t, a_t) = R_{\theta_i}(s_t, a_t) + \gamma T_{\xi_i}(s_t, a_t), \quad i = 1, 2$$
$$Q'_{\phi_i}(s_{t+1}, a_{t+1}) = R'_{\theta_i}(s_{t+1}, a_{t+1}) + \gamma T'_{\xi_i}(s_{t+1}, a_{t+1}), \quad i = 1, 2 \quad (6)$$

where R_{θ_i} and T_{ξ_i} are RPN and QRN, R'_{θ_i} and T'_{ξ_i} are target RPN and QRN, respectively. We use separate MLPs to model the RPN and QRN.

Since the distribution of live-stream (short video) watch time changes drastically over time, the time gain reward r in Eq. 2 becomes difficult to learn. In this work, we propose a *distribution discretization* method to improve reward learning.

Formally, we divide the live-stream and short video watch time distribution into N_l and N_v non-overlapping bins, where each bin represents an interval of live-stream (short video) watch time. Let y denote the actual live-stream or short video watch time, which falls into the time bin $[y_{st}, y_{end}]$. The proportion of y within this bin is $\delta = \frac{y - y_{st}}{y_{end} - y_{st}} \in [0, 1]$. Then, we have a *linear reconstruction layer* to reconstruct y from δ:

$$y = y_{st} + \delta \cdot (y_{end} - y_{st}) \quad (7)$$

which resembles the structure of linear reward shifting [35].

Let $o(t)_l \in \mathbb{R}^{N_l+1}$, $o(t)_v \in \mathbb{R}^{N_v+1}$ be one-hot vectors representing the time bins in which the real live-stream (short video) watch time of sample (s_t, a_t, r_t) falls. Note that a separate bin is set for the case $a_t = 0$. Then, the RPN R_{θ_i} can be modeled by multi-task neural networks:

$$R_{\theta_i}(s_t, a_t) = sigmoid\left(F_{\Gamma_i}(s_t, a_t) - G_{\Theta_i}(s_t, a_t)\right)$$
$$F_{\Gamma_i}(s_t, a_t) = o(t)_l^T \left(y_l^{st} + f_{\Gamma_i}(s_t, a_t) \cdot \left(y_l^{end} - y_l^{st}\right)\right) \quad (8)$$
$$G_{\Theta_i}(s_t, a_t) = o(t)_v^T \left(y_v^{st} + g_{\Theta_i}(s_t, a_t) \cdot \left(y_v^{end} - y_v^{st}\right)\right)$$

where $y_l^{st}, y_l^{end} \in \mathbb{R}^{N_l+1}$ predefined left (right) boundary vectors for the live-stream watch time bin, $y_v^{st}, y_v^{end} \in \mathbb{R}^{N_v+1}$ are predefined left (right) boundary vectors for the short video watch time bin. Note that introducing the posterior one-hot vectors $o(t)_l$ and $o(t)_v$ in Eq. 8 will not affect the calculation of $Q'_{\phi_i}(s_{t+1}, \cdot)$, because we have already reserved r_{t+1} in the dataset $\mathcal{D}$. Therefore, $o(t+1)_l$ and $o(t+1)_v$ can be easily obtained from r_{t+1} to compute $R'_{\theta_i}(s_{t+1}, \cdot)$.

As shown in Eq. 8, we employ two separate MLPs, $f_{\Gamma_i}(s_t, a_t)$ and $g_{\Theta_i}(s_t, a_t)$, to predict the proportions within a time bin. We then reconstruct the predicted live-stream and short video watch times, $F_{\Gamma_i}(s_t, a_t)$ and $G_{\Theta_i}(s_t, a_t)$, respectively. Finally, we obtain the predicted normalized reward, $R_{\theta_i}(s_t, a_t)$. To optimize the predicted watch time proportions, we use Huber Loss as follows:

$$\mathcal{L}_{SL} = \sum_{i=1}^{2} Huber\_Loss(\delta_l, F'_{\Gamma_i}) + Huber\_Loss(\delta_v, G'_{\Theta_i}) \quad (9)$$

where δ_l, δ_v are the actual proportion labels for live-stream and short video watch times, respectively.

The reason for using Huber loss on the time proportion δ instead of the actual watch time y is that the time proportion lies within the range $[0, 1]$, which results in smaller gradients in the neural network. Additionally, the variance of δ is much smaller than that of the original watch time y. Consequently, the outputs of the learned reward networks (f_{Γ_i} and g_{Θ_i}) will exhibit smaller variances. Hence, reward learning with the discretization of watch time distributions can be viewed as a novel *variance reduction* technique.

3.3.3 Actor Network. We also incorporate the multi-group state decomposition module into the actor network. The loss function of the actor network is shown below:

$$\mathcal{L}_{Actor} = \mathbb{E}_{(s,a) \in \mathcal{D}} \left[-\hat{Q}(s_t, a_t) \log p(s_t, a_t)\right] \quad (10)$$

where $\hat{Q}(s_t, a_t) = \min_{i=1,2} Q_{\phi_i}(s_t, a_t)$, and $p(s_t, a_t)$ is the action probability output of the actor network.

Moreover, we observe that large values of $\hat{Q}(s_t, a_t)$ may cause instability in actor training, which can ultimately lead to *policy deterioration*, where $\forall t$, $\pi(a_t = 1|s_t) > \pi(a_t = 0|s_t)$ or $\pi(a_t = 1|s_t) < \pi(a_t = 0|s_t)$. To address this, we apply softmax normalization to $\hat{Q}(s_t, a_t)$ to obtain $\hat{Q}_{norm} = softmax(\hat{Q}(s_t, a_t))$, and propose a modified actor loss function:

$$\mathcal{L}_{Actor} = \mathbb{E}_{(s,a) \in \mathcal{D}} \left[-\hat{Q}_{norm}(s_t, a_t) \log p(s_t, a_t)\right] \quad (11)$$

A similar loss function can be found in AWAC [32], and its theoretical results demonstrate that the above loss is equivalent to an implicitly constrained RL problem:

$$\pi_{k+1} = \arg\max_{\pi \in \Pi} \mathbb{E}_{a \sim \pi(\cdot|s)} \left[\hat{Q}^{\pi_k}(s_t, a_t)\right]$$
$$\text{s.t. } D_{KL}\left(\pi(\cdot|s)\|\pi_o(\cdot|s)\right) \leq \epsilon \quad (12)$$

where D_{KL} is the Kullback-Leibler (KL) divergence, and π_o is the behavior policy derived from the dataset $\mathcal{D}$.

We note that the actor loss in Eq. 11 is a standard cross-entropy loss function. From the perspective of knowledge distillation [17], the actor distills policy knowledge from more complex critic networks. The teacher critic networks guide the more lightweight student actor network to adjust and converge to an optimal policy. In practice, we only need to deploy the actor network in the online live-stream recommendation system, which significantly reduces computational complexity and improves real-time respond speed.

Overall, the final loss function of our proposed SL-MGAC algorithm is as follows:

$$\mathcal{L} = \mathcal{L}_{Actor} + \mathcal{L}_{Critic} + \mathcal{L}_{SL} \quad (13)$$

3.4 Online Exploration and Deployment

For online exploration, we adopt the commonly used ϵ-greedy [42] strategy:

$$\pi_{online}(s_t) = \begin{cases} \text{random action from } \mathcal{A}(s_t), & if \ \psi < \epsilon \\ \arg\max_{a \in \mathcal{A}(s_t)} \pi(a_t|s_t), & \text{otherwise} \end{cases} \quad (14)$$

where ψ is a random number, and ϵ is maximal exploration probability.

We deploy the SL-MGAC algorithm in our recommendation system, and the overall system architecture is shown in Fig. 4. The online RL agent collects real-time user interaction logs, while the offline model trainer optimizes the SL-MGAC model in an off-policy manner using streaming training data. Moreover, the offline trainer sends the latest model parameters to update the online deployed actor network in real-time.
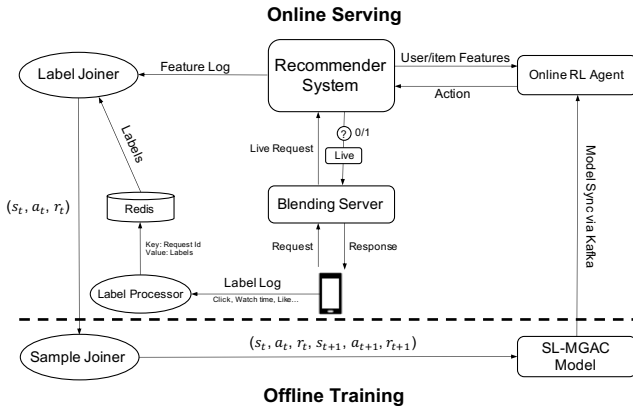

Figure 4: System Architecture of the SL-MGAC algorithm.

4 Experiments

We conduct both offline evaluation on a real-world dataset collected from our recommendation system and online A/B test experiments with SL-MGAC and the baselines.

4.1 Dataset

Due to the lack of publicly available datasets for recommendation decisions involving live-streaming injections in short video feeds, we collect a dataset from our recommendation system with 10,000 users through random sampling over a full day, ensuring that the proportions of different user groups are similar to those in real online data. In total, we have over 180,000 samples, which are split into training and test sets with a 4:1 ratio.

4.2 Compared Methods

4.2.1 Baselines. We compare our approach with existing non-reinforcement learning and reinforcement learning methods.

- **Learning to Rank (L2R)** [5]. A supervised learning framework that predicts the reward for each action. The action with the maximum reward is selected as the agent's action.
- **DQN** [31]. A deep neural network algorithm for Q-learning that introduces the technique of target network updates.

- **BCQ** [13]. A widely used offline reinforcement learning algorithm that adds action restrictions and encourages the agent to behave similarly to the behavior policy.
- **SAC** [6, 15]. A classic off-policy reinforcement learning method that maximizes the trade-off between cumulative reward and policy entropy. We use the discrete version of SAC in later experiments.
- **TD3** [12]. A modified version of DDPG [26] that addresses function approximation errors using three techniques: Clipped Double Q-Learning, Delayed Policy Updates, and Target Policy Smoothing.
- **TD3-BC** [11]. An offline reinforcement learning variant of the TD3 algorithm, with behavior cloning (BC) regularization to constrain policy learning.
- **IQL** [22]. An offline reinforcement learning algorithm that leverages expectile regression in Q-Learning.

Note that in our optimal live-stream injection control problem, the action is discrete. Therefore, we introduce the Straight-Through Gumbel Softmax [20] technique into TD3 and TD3-BC.

4.2.2 Variations of our model. We also compare the SL-MGAC algorithm with several variants in an ablation study to illustrate the effectiveness of multi-group state decomposition, supervised learning for critic learning, distribution discretization (DD), and other techniques.

- **SL-MGAC (w/o MG)**: An SL-MGAC variant without the Multi-Group State Decomposition module.
- **SL-MGAC (w/o MG & DD)**: An SL-MGAC variant without the Multi-Group State Decomposition module and the distribution discretization technique in reward learning.
- **SL-MGAC (w/o MG & DD & SL)**: An SL-MGAC variant without the Multi-Group State Decomposition module, the distribution discretization technique in reward learning, and the supervised learning procedure.
- **SL-MGAC (w/o LN)**: An SL-MGAC variant without the Layer Normalization technique.
- **SL-MGAC (w/o SG)**: An SL-MGAC variant without the Stop Gradient technique for hidden state representation in the actor network.
- **SL-MGAC (w/o Q-norm)**: An SL-MGAC variant without Q value normalization in the actor loss.
- **SL-MGAC-0**: An SL-MGAC variant with the discount factor $\gamma = 0$.
- **SL-MGAC-sep**: An SL-MGAC variant with separate optimization of the actor network. Hence, $\hat{Q}_{norm}$ in Eq. 11 is detached from the computation graph.
- **SL-MGAC-vanilla**: An SL-MGAC variant with the vanilla Q label in the critic loss, as shown below, where $p(s_{t+1}, \cdot)$ is the action probability of s_{t+1} output by the actor network.

$$Q_{label}(s_{t+1}) = r(s_t, a_t) + \gamma \sum_{a_{t+1}} p(s_{t+1}, a_{t+1})\hat{Q}(s_{t+1}, a_{t+1}) \quad (15)$$

4.3 Implementation Details

To ensure fairness among all compared methods, we use a consistent feature extraction module with an embedding layer of size 5000. In addition to the embedding layer, the feature extraction

module includes a 2-layer MLP with hidden sizes of [256, 128]. The batch size and number of epochs for all methods are 2048 and 500, respectively. The learning rate for the embedding layer is set to 1e-5, while the learning rate for other hidden parameters is 1e-3. The discount factor γ is set to 0.9 for all methods. The detailed network architecture and parameter settings for SL-MGAC are provided in Table 4 of Appendix B.

4.4 Offline Policy Evaluation

We follow the approach in [44] and adopt a commonly used offline policy evaluation method, namely Normalized Capped Importance Sampling (NCIS) [37], to evaluate performance. The evaluation metric is the cumulative reward across all trajectories of test users. Note that the reward for each sample is defined in Eq. 3.

Methods	Cumulative Reward
L2R [5]	413.49
DQN [31]	413.18
BCQ [13]	416.69
SAC [6]	**435.41**
TD3 [12]	432.08
TD3-BC [11]	430.23
IQL [22]	432.03
SL-MGAC-sep	435.19
SL-MGAC-vanilla	450.21
SL-MGAC	**458.49**

Table 1: Overall offline performance of compared methods.

The offline policy evaluation results are shown in Table 1. Compared to the supervised learning method L2R, most RL methods achieve higher cumulative rewards, except for DQN. SL-MGAC significantly outperforms all other methods, demonstrating that SL-MGAC can achieve higher long-term rewards in the complex live-stream & short video mixed recommendation system with drastically changing data distributions. Furthermore, SL-MGAC outperforms SL-MGAC-vanilla, suggesting that incorporating the actor network in the Q label calculation of Eq. 15 may interfere with critic learning to some extent, slightly affecting the performance of SL-MGAC-vanilla. Additionally, SL-MGAC converges faster than SL-MGAC-sep during training, as shown in Fig. 8 in Appendix C, and achieves a higher cumulative reward in offline evaluation. This may be due to the information loss caused by detaching $\hat{Q}_{norm}$, which can lead to slower convergence for SL-MGAC-sep.

4.5 Ablation Study

We compare the offline performance of different SL-MGAC variants. As shown in Table 2, SL-MGAC outperforms all other variants on our offline dataset, demonstrating the effectiveness of the proposed multi-group state decomposition module, supervised learning procedure, and other techniques. Moreover, we find that SL-MGAC (w/o Q-norm) achieves the lowest reward, indicating that the Q-normalization technique in the actor loss enhances the model's convergence and improves its performance.

Next, we compare the training processes of SL-MGAC and SL-MGAC (w/o MG), as shown in Fig. 5. We observe that the Q-value

Methods	Cumulative Reward
SL-MGAC (w/o MG)	454.62
SL-MGAC (w/o MG & DD)	452.59
SL-MGAC (w/o MG & DD & SL)	449.13
SL-MGAC (w/o LN)	453.61
SL-MGAC (w/o SG)	457.26
SL-MGAC (w/o Q-norm)	392.12
SL-MGAC	**458.49**

Table 2: Offline performance of SL-MGAC variants.

curve of SL-MGAC is more stable than that of SL-MGAC (w/o MG), and the Q-value variance of SL-MGAC is much smaller. This demonstrates the effectiveness and variance reduction effect of the MG-SD module.
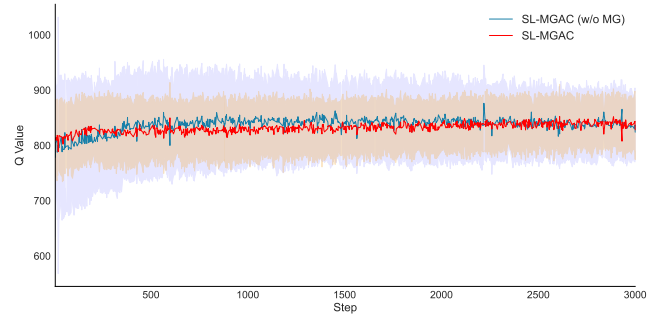

Figure 5: The Q value curves between SL-MGAC and SL-MGAC (w/o MG) over 10 rounds of training. The lines correspond to the means of Q-value and the shaded areas correspond to the standard deviations.

4.6 Parameter Sensitivity

We analyze the impact of the number of user groups K on the performance of SL-MGAC. As shown in Fig. 6, the proposed SL-MGAC algorithm with $K = 6$ achieves the highest cumulative reward, demonstrating that increasing the number of user groups within a certain range improves model performance.
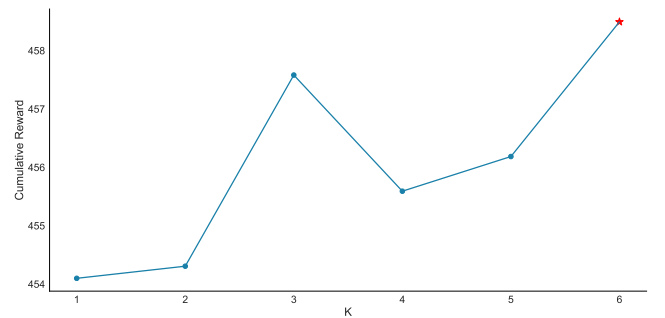

Figure 6: Performance of different numbers of user group K.

4.7 Online A/B Test Experiment

We compare the improvements of different methods in terms of live-stream daily active users (DAU) and watch time relative to the baseline. The baseline uses the SAC framework for online live-stream injection. The online A/B test results are shown in Table 3. SL-MGAC achieves the largest improvement in live-stream watch time while also increasing live-stream DAU. Although SL-MGAC-0 shows a larger improvement in live-stream DAU compared to SL-MGAC, it tends to be more greedy in injecting live-streams, which may negatively impact the long-term user experience for most users. Therefore, this demonstrates that SL-MGAC is more effective in maximizing long-term rewards when injecting live-streams in response to user requests.

Methods	Live-stream DAU	Live-stream Watch Time
L2R	+0.321%	-0.558%
SL-MGAC-0	**+3.928%**	-2.934%
SL-MGAC	+2.616%	**+7.431%**

Table 3: Online A/B Test Performance of compared methods.

Since the scale of live-stream supply and user interaction behaviors change drastically over time, more streamers tend to broadcast live during peak hours. As shown in Fig. 9 in Appendix C, SL-MGAC can adaptively adjust the live-stream injection strategy to increase live-stream exposure during peak hours, while reducing exposure during low-traffic periods.

4.8 Online Model Stability

We evaluate the online model stability between the SAC-based baseline and SL-MGAC. As shown in Fig. 7, the live-stream injection ratio fluctuates drastically throughout the day for both models. However, SL-MGAC exhibits greater stability than the baseline, with a smaller amplitude. Note that the live-stream injection ratio refers to the proportion of requests with action $a = 1$.
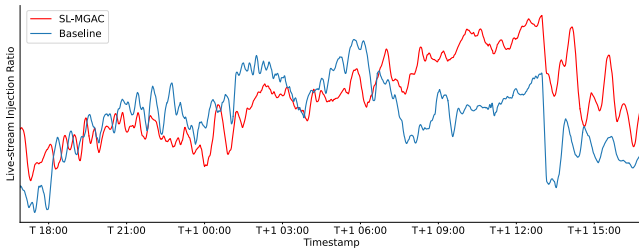

Figure 7: The trend curve of online live-stream injection ratio during a whole day.

We calculate the amplitudes of the live-stream injection ratio within sliding time windows of 20 minutes. The amplitude density is shown in Fig. 10 in Appendix C. The results indicate that SL-MGAC has a smaller mean amplitude and fewer outliers. In contrast, the baseline model exhibits larger amplitude outliers, as highlighted in the red dashed box, which demonstrates the superior online model stability of SL-MGAC.

5 Related Work

5.1 RL in Recommendation Systems

Reinforcement learning (RL) aims to optimize long-term cumulative rewards over time, which has attracted significant attention in recommendation systems research in recent years [1]. Methods such as SLATEQ [18], GeMS [8], and HAC [27] use RL to recommend entire item lists, where the number of candidate items can be large. BatchRL-MTF [47], RLUR [4], and UNEX-RL [46] leverage RL to model the multi-rank score aggregation process, optimizing the weights for score aggregation. The work in [29] explores the use of off-policy RL for multi-session personalized search ranking. Cross-DQN [25] introduces a RL-based approach for ad allocation in a feed, aiming to maximize revenue while improving user experience. Additionally, traditional RL methods such as DQN [30, 31], Double DQN [40], SAC [15], DDPG [26], and TD3 [12] serve as backbones in real-world RL applications for recommendation systems.

A similar approach, called self-supervised actor-critic [43], combines supervised learning with critic learning. Their supervised learning task focuses on predicting the next item recommendation probability, whereas our approach introduces supervised learning to restrict critic learning.

5.2 RL divergence and instability

Recently, there has been growing literature focusing on RL divergence and instability. [40] introduces Double DQN to mitigate the *maximization bias* problem in DQN. [12] proposes the Clipped Double Q-Learning technique in TD3 to reduce the overestimation of Q-values. [28] introduces a bias-free, input-dependent baseline for the policy gradient algorithm [36] to reduce variance and improve training stability. [9] investigates policy collapse in a 2-state MDP and finds that L2 regularization and the non-stationary Adam optimizer [21] are both effective in alleviating RL instability. [45] theoretically analyzes the causes of RL divergence and applies Layer Normalization to mitigate RL divergence and instability.

6 Conclusion

In this work, we propose a novel Supervised Learning-enhanced Multi-Group Actor-Critic algorithm (SL-MGAC) to optimize request-level live-stream injection policies in the challenging context of a live-stream & short video mixed recommendation system. Unlike existing RL methods for recommendation systems, our approach focuses on enhancing the stability and robustness of the RL model. Specifically, we introduce a multi-group state decomposition module to reduce prediction variance and seamlessly integrate multi-task reward learning with traditional critic learning to constrain Q-value estimation. In practice, we aim to minimize the risk of *policy deterioration* or *model collapse*, thereby enabling the proposed SL-MGAC method to be successfully deployed in large-scale industrial recommendation systems.

7 Acknowledgment

References

[1] M Mehdi Afsar, Trafford Crump, and Behrouz Far. 2022. Reinforcement learning based recommender systems: A survey. *Comput. Surveys* 55, 7 (2022), 1–38.

[2] Oron Anschel, Nir Baram, and Nahum Shimkin. 2017. Averaged-dqn: Variance reduction and stabilization for deep reinforcement learning. In *International conference on machine learning*. PMLR, 176–185.

[3] Jimmy Lei Ba. 2016. Layer normalization. *arXiv preprint arXiv:1607.06450* (2016).

[4] Qingpeng Cai, Shuchang Liu, Xueliang Wang, Tianyou Zuo, Wentao Xie, Bin Yang, Dong Zheng, Peng Jiang, and Kun Gai. 2023. Reinforcing user retention in a billion scale short video recommender system. In *Companion Proceedings of the ACM Web Conference 2023*. 421–426.

[5] Ming Chen and Xiuze Zhou. 2020. DeepRank: Learning to rank with neural networks for recommendation. *Knowledge-Based Systems* 209 (2020), 106478.

[6] Petros Christodoulou. [n. d.]. Soft actor-critic for discrete action settings. arXiv 2019. *arXiv preprint arXiv:1910.07207* ([n. d.]).

[7] Vibhavari Dasagi, Jake Bruce, Thierry Peynot, and Jürgen Leitner. 2019. Ctrl-z: Recovering from instability in reinforcement learning. *arXiv preprint arXiv:1910.03732* (2019).

[8] Romain Deffayet, Thibaut Thonet, Jean-Michel Renders, and Maarten De Rijke. 2023. Generative slate recommendation with reinforcement learning. In *Proceedings of the Sixteenth ACM International Conference on Web Search and Data Mining*. 580–588.

[9] Shibhansh Dohare, Qingfeng Lan, and A Rupam Mahmood. 2023. Overcoming policy collapse in deep reinforcement learning. In *Sixteenth European Workshop on Reinforcement Learning*.

[10] Vincent François-Lavet, Raphael Fonteneau, and Damien Ernst. 2015. How to discount deep reinforcement learning: Towards new dynamic strategies. *arXiv preprint arXiv:1512.02011* (2015).

[11] Scott Fujimoto and Shixiang Shane Gu. 2021. A minimalist approach to offline reinforcement learning. *Advances in neural information processing systems* 34 (2021), 20132–20145.

[12] Scott Fujimoto, Herke Hoof, and David Meger. 2018. Addressing function approximation error in actor-critic methods. In *International conference on machine learning*. PMLR, 1587–1596.

[13] Scott Fujimoto, David Meger, and Doina Precup. 2019. Off-policy deep reinforcement learning without exploration. In *International conference on machine learning*. PMLR, 2052–2062.

[14] Evan Greensmith, Peter L Bartlett, and Jonathan Baxter. 2004. Variance Reduction Techniques for Gradient Estimates in Reinforcement Learning. *Journal of Machine Learning Research* 5, 9 (2004).

[15] Tuomas Haarnoja, Aurick Zhou, Pieter Abbeel, and Sergey Levine. 2018. Soft actor-critic: Off-policy maximum entropy deep reinforcement learning with a stochastic actor. In *International conference on machine learning*. PMLR, 1861–1870.

[16] Trevor Hastie, Robert Tibshirani, Jerome H Friedman, and Jerome H Friedman. 2009. *The elements of statistical learning: data mining, inference, and prediction*. Vol. 2. Springer.

[17] Geoffrey Hinton. 2015. Distilling the Knowledge in a Neural Network. *arXiv preprint arXiv:1503.02531* (2015).

[18] Eugene Ie, Vihan Jain, Jing Wang, Sanmit Narvekar, Ritesh Agarwal, Rui Wu, Heng-Tze Cheng, Tushar Chandra, and Craig Boutilier. 2019. SlateQ: A tractable decomposition for reinforcement learning with recommendation sets. (2019).

[19] Arthur Jacot, Franck Gabriel, and Clément Hongler. 2018. Neural tangent kernel: Convergence and generalization in neural networks. *Advances in neural information processing systems* 31 (2018).

[20] Eric Jang, Shixiang Gu, and Ben Poole. 2016. Categorical reparameterization with gumbel-softmax. *arXiv preprint arXiv:1611.01144* (2016).

[21] Diederik P Kingma. 2014. Adam: A method for stochastic optimization. *arXiv preprint arXiv:1412.6980* (2014).

[22] Ilya Kostrikov, Ashvin Nair, and Sergey Levine. 2021. Offline reinforcement learning with implicit q-learning. *arXiv preprint arXiv:2110.06169* (2021).

[23] Aviral Kumar, Justin Fu, Matthew Soh, George Tucker, and Sergey Levine. 2019. Stabilizing off-policy q-learning via bootstrapping error reduction. *Advances in neural information processing systems* 32 (2019).

[24] Yuxi Li. 2017. Deep reinforcement learning: An overview. *arXiv preprint arXiv:1701.07274* (2017).

[25] Guogang Liao, Ze Wang, Xiaoxu Wu, Xiaowen Shi, Chuheng Zhang, Yongkang Wang, Xingxing Wang, and Dong Wang. 2022. Cross dqn: Cross deep q network for ads allocation in feed. In *Proceedings of the ACM Web Conference 2022*. 401–409.

[26] TP Lillicrap. 2015. Continuous control with deep reinforcement learning. *arXiv preprint arXiv:1509.02971* (2015).

[27] Shuchang Liu, Qingpeng Cai, Bowen Sun, Yuhao Wang, Ji Jiang, Dong Zheng, Peng Jiang, Kun Gai, Xiangyu Zhao, and Yongfeng Zhang. 2023. Exploration and regularization of the latent action space in recommendation. In *Proceedings of the ACM Web Conference 2023*. 833–844.

[28] Hongzi Mao, Shaileshh Bojja Venkatakrishnan, Malte Schwarzkopf, and Mohammad Alizadeh. 2018. Variance reduction for reinforcement learning in input-driven environments. *arXiv preprint arXiv:1807.02264* (2018).

[29] Dadong Miao, Yanan Wang, Guoyu Tang, Lin Liu, Sulong Xu, Bo Long, Yun Xiao, Lingfei Wu, and Yunjiang Jiang. 2021. Sequential Search with Off-Policy Reinforcement Learning. In *Proceedings of the 30th ACM International Conference on Information & Knowledge Management*. 4006–4015.

[30] Volodymyr Mnih. 2013. Playing atari with deep reinforcement learning. *arXiv preprint arXiv:1312.5602* (2013).

[31] Volodymyr Mnih, Koray Kavukcuoglu, David Silver, Andrei A Rusu, Joel Veness, Marc G Bellemare, Alex Graves, Martin Riedmiller, Andreas K Fidjeland, Georg Ostrovski, et al. 2015. Human-level control through deep reinforcement learning. *nature* 518, 7540 (2015), 529–533.

[32] Ashvin Nair, Abhishek Gupta, Murtaza Dalal, and Sergey Levine. 2020. Awac: Accelerating online reinforcement learning with offline datasets. *arXiv preprint arXiv:2006.09359* (2020).

[33] Martin L Puterman. 1990. Markov decision processes. *Handbooks in operations research and management science* 2 (1990), 331–434.

[34] Joshua Romoff, Peter Henderson, Alexandre Piché, Vincent Francois-Lavet, and Joelle Pineau. 2018. Reward estimation for variance reduction in deep reinforcement learning. *arXiv preprint arXiv:1805.03359* (2018).

[35] Hao Sun, Lei Han, Rui Yang, Xiaoteng Ma, Jian Guo, and Bolei Zhou. 2022. Exploit reward shifting in value-based deep-rl: Optimistic curiosity-based exploration and conservative exploitation via linear reward shaping. *Advances in neural information processing systems* 35 (2022), 37719–37734.

[36] Richard S Sutton, David McAllester, Satinder Singh, and Yishay Mansour. 1999. Policy gradient methods for reinforcement learning with function approximation. *Advances in neural information processing systems* 12 (1999).

[37] Adith Swaminathan and Thorsten Joachims. 2015. The self-normalized estimator for counterfactual learning. *advances in neural information processing systems* 28 (2015).

[38] Chen Tessler, Daniel J Mankowitz, and Shie Mannor. 2018. Reward constrained policy optimization. *arXiv preprint arXiv:1805.11074* (2018).

[39] Masatoshi Uehara, Chengchun Shi, and Nathan Kallus. 2022. A review of off-policy evaluation in reinforcement learning. *arXiv preprint arXiv:2212.06355* (2022).

[40] Hado Van Hasselt, Arthur Guez, and David Silver. 2016. Deep reinforcement learning with double q-learning. In *Proceedings of the AAAI conference on artificial intelligence*, Vol. 30.

[41] A Vaswani. 2017. Attention is all you need. *Advances in Neural Information Processing Systems* (2017).

[42] Christopher John Cornish Hellaby Watkins. 1989. Learning from delayed rewards. (1989).

[43] Xin Xin, Alexandros Karatzoglou, Ioannis Arapakis, and Joemon M Jose. 2020. Self-supervised reinforcement learning for recommender systems. In *Proceedings of the 43rd International ACM SIGIR conference on research and development in Information Retrieval*. 931–940.

[44] Wanqi Xue, Qingpeng Cai, Zhenghai Xue, Shuo Sun, Shuchang Liu, Dong Zheng, Peng Jiang, Kun Gai, and Bo An. 2023. PrefRec: recommender systems with human preferences for reinforcing long-term user engagement. In *Proceedings of the 29th ACM SIGKDD Conference on Knowledge Discovery and Data Mining*. 2874–2884.

[45] Yang Yue, Rui Lu, Bingyi Kang, Shiji Song, and Gao Huang. 2024. Understanding, predicting and better resolving Q-value divergence in offline-RL. *Advances in Neural Information Processing Systems* 36 (2024).

[46] Gengrui Zhang, Yao Wang, Xiaoshuang Chen, Hongyi Qian, Kaiqiao Zhan, and Ben Wang. 2024. UNEX-RL: Reinforcing Long-Term Rewards in Multi-Stage Recommender Systems with UNidirectional EXecution. In *Proceedings of the AAAI Conference on Artificial Intelligence*, Vol. 38. 9305–9313.

[47] Qihua Zhang, Junning Liu, Yuzhuo Dai, Yiyan Qi, Yifan Yuan, Kunlun Zheng, Fan Huang, and Xianfeng Tan. 2022. Multi-task fusion via reinforcement learning for long-term user satisfaction in recommender systems. In *Proceedings of the 28th ACM SIGKDD conference on knowledge discovery and data mining*. 4510–4520.

[48] Yu Zhang and Qiang Yang. 2021. A survey on multi-task learning. *IEEE transactions on knowledge and data engineering* 34, 12 (2021), 5586–5609.

[49] Guorui Zhou, Xiaoqiang Zhu, Chenru Song, Ying Fan, Han Zhu, Xiao Ma, Yanghui Yan, Junqi Jin, Han Li, and Kun Gai. 2018. Deep interest network for click-through rate prediction. In *Proceedings of the 24th ACM SIGKDD international conference on knowledge discovery & data mining*. 1059–1068.

[50] Lixin Zou, Long Xia, Zhuoye Ding, Jiaxing Song, Weidong Liu, and Dawei Yin. 2019. Reinforcement learning to optimize long-term user engagement in recommender systems. In *Proceedings of the 25th ACM SIGKDD international conference on knowledge discovery & data mining*. 2810–2818.

A Proof of Theorem 3.1

PROOF. Let state space $\mathcal{S} = \bigcup_{i=1}^{K} \mathcal{S}_i, \forall i \neq j \; \mathcal{S}_i \cap \mathcal{S}_j = \varnothing$, state $s \in \mathcal{S}$. Let r be the real reward of state s and action a, $\hat{r}$ be the predicted value of r over $\mathcal{S}$, $\hat{r}_i$ be the predicted reward of r over $\mathcal{S}_i$.

Since a user has at most one request at timestamp t, a user will have at most one state s. We assume the state count N of $\mathcal{S}$ is finite, the state count of $\mathcal{S}_i$ is N_i. Let μ be the mean value of $\hat{r}$ over $\mathcal{S}$, μ_i be the mean value of $\hat{r}_i$ over $\mathcal{S}_i$, then we have:

$$
\begin{aligned}
Var[\hat{r}] &= \frac{1}{N} \sum_{j=1}^{N} \left(\hat{r}_j - \mu \right)^2 \\
&= \frac{1}{N} \sum_{i=1}^{K} \sum_{j=1}^{N_i} \left(\hat{r}_{ij} - \mu \right)^2 \\
&= \frac{1}{N} \sum_{i=1}^{K} \sum_{j=1}^{N_i} \left(\hat{r}_{ij} - \mu_i + \mu_i - \mu \right)^2 \\
&= \frac{1}{N} \sum_{i=1}^{K} \sum_{j=1}^{N_i} \left(\hat{r}_{ij} - \mu_i \right)^2 + \frac{1}{N} \sum_{i=1}^{K} N_i \left(\mu_i - \mu \right)^2
\end{aligned}
\tag{16}
$$

where the first term is within-class variance $Var_a[\hat{r}]$ and the second term is between-class variance $Var_b[\hat{r}]$. As $Var_b[\hat{r}] > 0$, we have

$$
Var[\hat{r}] > \frac{1}{N} \sum_{i=1}^{K} \sum_{j=1}^{N_i} \left(\hat{r}_{ij} - \mu_i \right)^2 = Var_a[\hat{r}]
\tag{17}
$$

As we partition the state space $\mathcal{S}$ into K disjoint sub-spaces $\mathcal{S}_i$, then the variance of a neural network f with multi-group state decomposition(MG SD) module is $Var_a[\hat{r}]$ while the variance of a neural network f' without MG-SD module is $Var[\hat{r}]$. □

B Tables

Hyper-parameter	Value
MGN in Actor	[128, 63, 31, 2]
MGN in RPN	[128, 64, 32, 8]
MGN in QRN	[128, 64, 32, 2]
Live-Time DDB	[0s, 6s, 15s, 30s, 60s, 100s, 600s, 1200s]
Video-Time DDB	[0s, 3s, 10s, 25s, 50s, 100s, 600s, 1200s]
Optimizer	Adam
User Group Number K	6
Online Exploration ϵ	0.2

Table 4: Hyper-parameters of SL-MGAC.

We denote MGN as the multi-group network, RPN as the Reward Prediction Network, QRN as Q Residual Networks, DDB as Distribution Discretization Bins. Both live and video watch time distribution have 7 time bins. We leave a separate time bin for the $a = 1$ case and hence the output layer dimension of RPN is 8.

C Figures

(a) Training Curves of Actor Loss

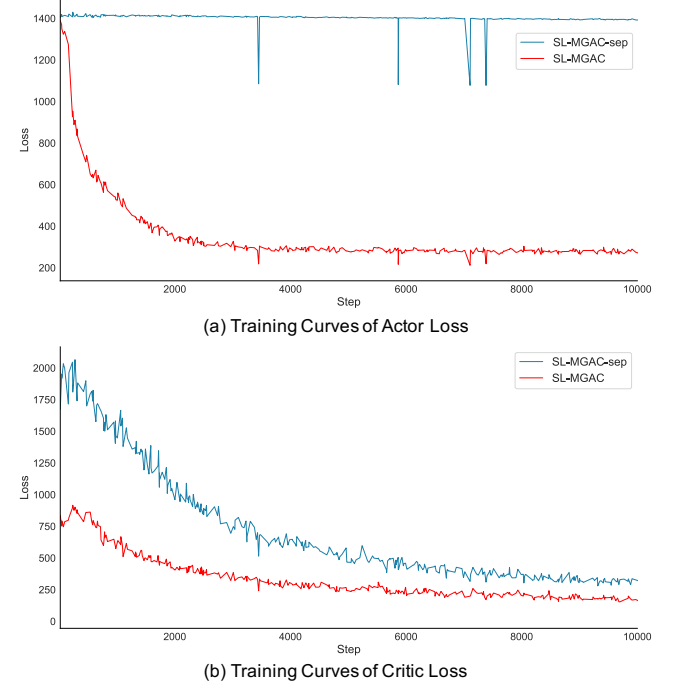(b) Training Curves of Critic Loss

Figure 8: Training Curves of SL-MGAC and SL-MGAC-sep.
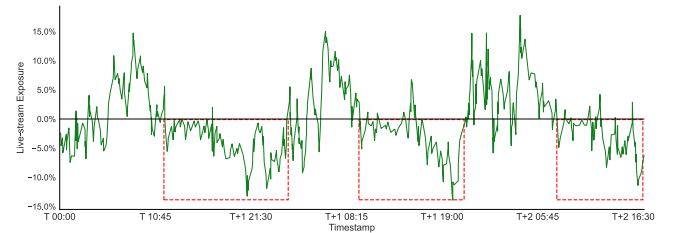

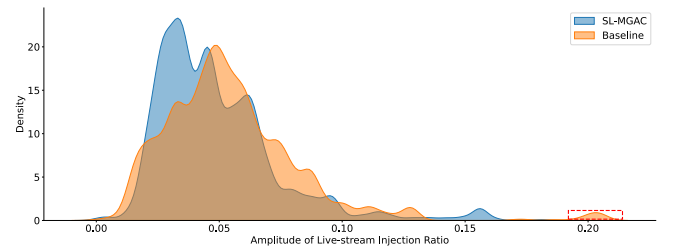Figure 9: Adaptive adjustments of live-stream exposure during peak hours and low-traffic periods.

Figure 10: The amplitude distribution of live-stream injection ratio.